Conf-780402--1

PREPRINT UCRL- 80374

Lawrence Livermore Laboratory

EFFECTS OF A HYPOTHETICAL LOSS-OF-COOLANT ACCIDENT ON A MARK I BOILING WATER REACTOR PRESSURE-SUPPRESSION SYSTEM

MASTER

J. H. Pitts and E. W. McCauley

December 22, 1977

This paper was prepared for submittal to the Proceedings of the 24th Annual Institute of Environmental Sciences Technical Meeting in Fort Worth, Texas, April 17-20, 1978.

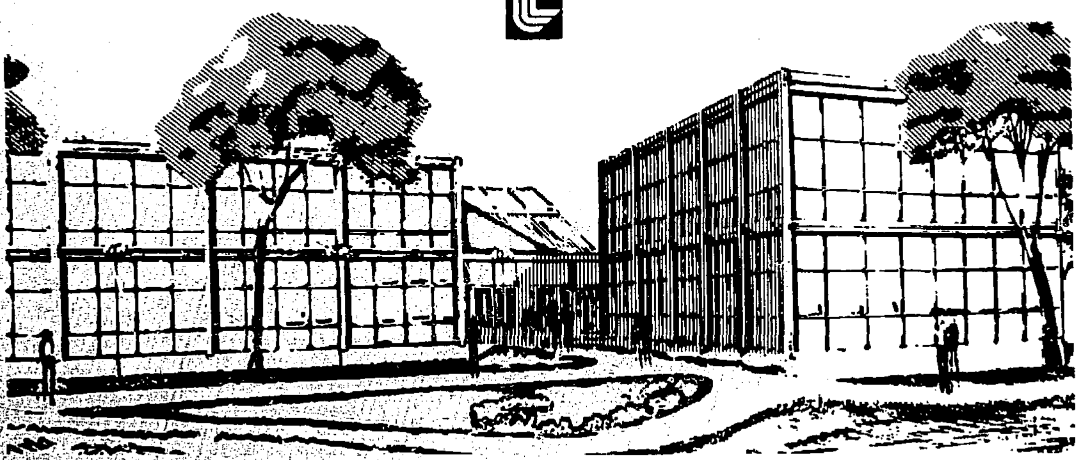

EFFECTS OF A HYPOTHETICAL LOSS-OF-COOLANT ACCIDENT ON A MARK I BOILING WATER REACTOR PRESSURE-SUPPRESSION SYSTEM

By: J. H. Pitts and E. W. McCauley
University of California, Lawrence Livermore Laboratory
P. O. Box 808, Livermore, CA 94550

AUTOBIOGRAPHY

Drs. Pitts and McCauley are principal investigators for the 1/5-scale, Mark I Boiling Water Reactor pressure-suppression experiment at Lawrence Livermore Laboratory (LLL). Under their direction, an accurate and versatile facility was constructed and air tests were completed in a period of 13 months.

Dr. Pitts received his education at Stanford University and at the University of California at Berkeley and Davis. He came to LLL in 1959 to participate in the successful "Pluto," nuclear-powered, ramjet program. He performed research in the field of nuclear propulsion until 1969 when he turned his attention to the flow of radioactive fluids through permeable earth formations. In 1976, he accepted his present position on the project described here.

Dr. McCauley received his Ph.D. in Nuclear Engineering from the University of Washington in 1967. Prior to this, he was an engineer and research group leader at Western Gear Corporation. He came to LLL in 1967 as a group leader in the nuclear space power program. He has worked extensively in the fields of fluid dynamics, gas dynamics, shock hydrodynamics, explosive analysis, related hazard assessment, and soil mechanics programming development. Presently he is leader of the Thermo Fluid Mechanics Engineering Group.

ABSTRACT

A loss-of-coolant accident (LOCA) in a boiling-water-reactor (BWR) power plant has never occurred. However, because this type of accident could be particularly severe, it is used as a principal theoretical basis for design. Under sponsorship of the U.S. Nuclear Regulatory Commission, we designed and constructed a complete three-dimensional experimental facility at Lawrence Livermore Laboratory. A series of consistent, versatile, and accurate air-water tests that simultate LOCA conditions has been completed on this 1/5-scale, Mark I BWR, pressure-suppression system. Results from these tests are used to quantify the vertical-loading function and to study the associated fluid dynamics phenomena. Detailed histories of vertical loads on the wetwell are shown. In particular, variation of hydrodynamic-generated vertical loads with changes in drywell-pressurization rate, downcomer submergence, and the vent-line loss coefficient are established. Initial drywell overpressure, which partially preclears the downcomers of water, substantially reduces the peak vertical loads. Scaling relationships, developed from dimensional analysis and verified by bench-top experiments, allow the 1/5-scale results to be applied to a full-scale BWR power plant. This analysis leads to dimensionless groupings that are invariant. These groupings show that, if water is used as the working fluid, the magnitude of the forces in a scaled facility is reduced by the cube of the scale factor and occurs in a time reduced by the square root of the scale factor.

INTRODUCTION

A Mark I boiling-water-reactor (BWR) power plant consists basically of (a) a light-bulb-shaped vessel called a drywell that contains the reactor pressure vessel, (b) a toroidal wetwell, a torus about half-filled with water and connected to the drywell with eight vent pipes, and (c) conventional equipment associated with power conversion. The pressure-suppression system, associated with these first two items, is shown in cross section in Fig. 1. These particular dimensions are for the Peach Bottom plant (1), which we used as a reference for designing our 1/5-scale experimental facility. The Peach Bottom drywell and the top half of the toroidal wetwell are initially filled with air at ambient pressure and are connected by open-flow passages. In full-scale, the flow passages consist of eight 2-m-diam vent pipes that connect the drywell to a 1.5-m-diam ring-header. The ringheader is formed in the shape of a torus and is positioned inside the toroidal wetwell. Ninety-six downcomers are attached to the ringheader. The downcomers, 0.6 m in diameter, are positioned in pairs along the axis of the ringheader and have open bottoms that are submerged 1.2 m below the water surface. Spacing varies between downcomer pairs along the ringheader; downcomers are not present in regions where the vent pipes attach to the ring-header.

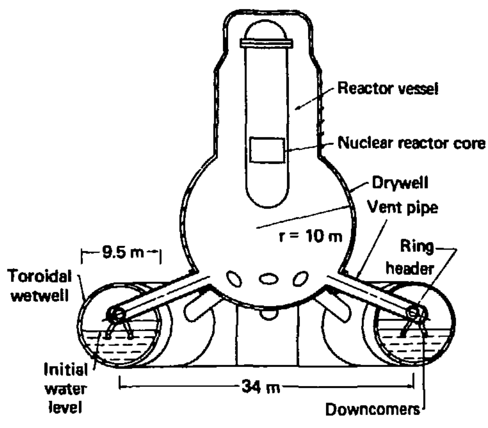

Figure 1. Cross section of a full-scale pressure-suppression system of a Mark I BWR power plant.

During a hypothetical loss-of-coolant accident (LOCA), a steam or recirculation line is assumed to break, and steam or water or both are discharged into the drywell. This results in injection of air, followed by steam, through the downcomers and into the toroidal wetwell. The steam condenses as it mixes with the water in the wetwell. Pressure inside both drywell and toroidal wetwell is kept below safe, containable limits.

We designed and constructed an accurate and versatile 1/5-scale model of the pressure-suppression system of the Peach Bottom plant (2). A series of 27, consistent and repeatable, air tests were completed. The primary purpose was to determine the history of vertical forces that occur on the pressure-suppression system during the initial phase of the hypothetical LOCA and to study the ensuing hydrodynamic phenomena.

The hydrodynamically generated loads produced in the injection process induce stresses in the structural components of the pressure-suppression system. Although the structural components are conservatively designed, large-scale experiments are desirable to verify predicted loads and to assure that adequate safety margins exist.

EXPERIMENTAL FACILITY

Primary components of the experimental facility include a bank of six nitrogen-storage vessels, a drywell, and 90-deg and 7.5-deg segments of the toroidal wetwell, as shown in Fig. 2. The nitrogen-storage vessels are connected to and pressurize the drywell at the desired rate for a particular test. This drywell-pressurization rate may be varied by changing the volume and initial pressure of the nitrogen-storage vessels. The volume of the drywell is scaled to properly supply both the 90-deg and 7.5-deg segments of the toroidal wetwell.

The 90-deg and 7.5-deg segments of the toroidal wetwell, including ringheaders and downcomers, are 1/5-scale, geometrical models of the Peach Bottom Nuclear Power Plant. A wall thickness of 19 mm ensures that the 1/5-scale toroidal wetwell is an essentially rigid structure. Figure 3 shows the 1/5-scale drywell and the 90-deg segment of the toroidal wetwell in cross section. Figure 4 is a photograph of the experimental facility. Design parameters are indicated in Table 1. A summary of instrumentation, including transducer accuracy and uncertainty specifications, is shown in Table 2. The 90-deg segment is supported externally with two trunnions at the transverse center and one auxiliary support at the bottom of one end. Each support contains a load cell. A three-point support system eliminates redundancy that could over-range the load cells as forces resulting from long-term thermal transients (e.g., diurnal temperature changes) develop.

Inside the 90-deg sector, the ringheader is connected to the toroidal wetwell by four vertical struts, in the same general fashion as the full-scale plant. Each of these four internal supports also contains a load cell. Redundancy in the ringheader-support system is eliminated by the inclusion of a flexible joint at the midplane of the ringheader. The 7.5-deg segment was included so that two-dimensional and three-dimensional effects could be compared during each test.

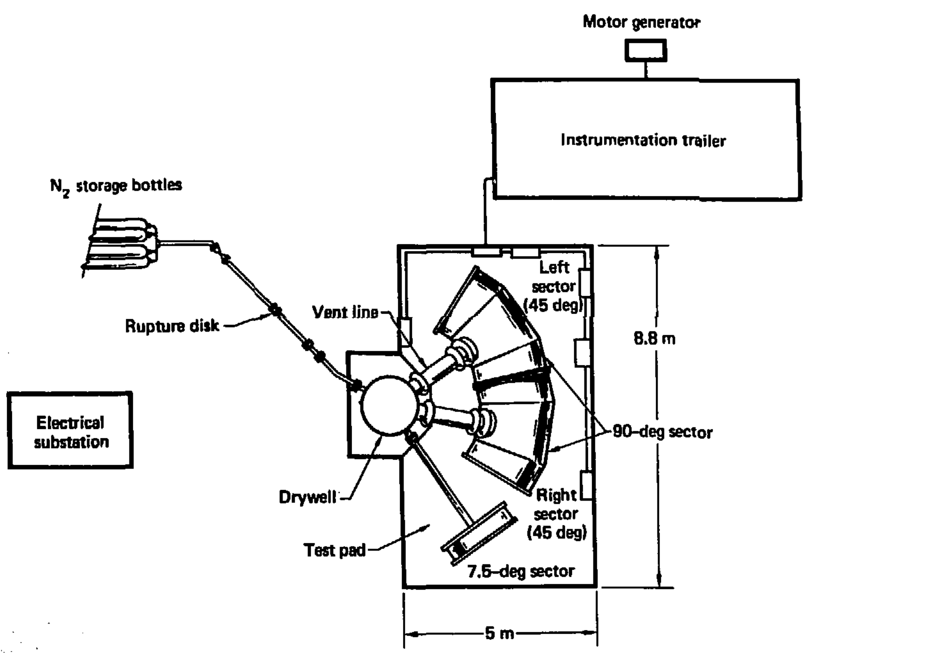

Figure 2. Schematic overhead view of the 1/5-scale experimental facility.

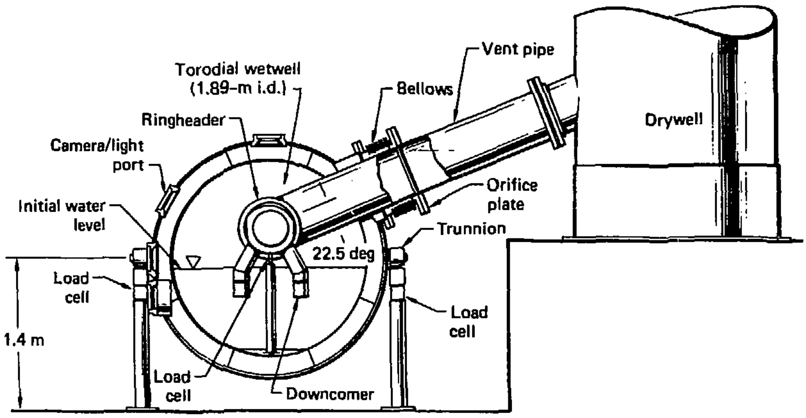

Figure 3. Cross section of the 1/5-scale experimental facility.

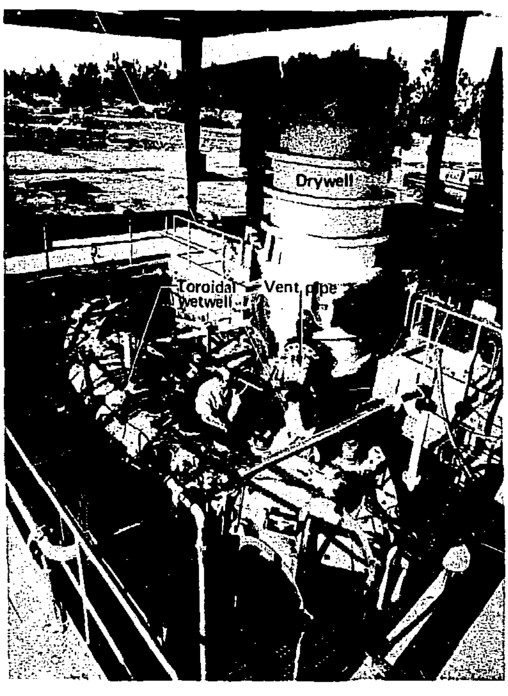

Figure 4. Photograph of the 1/5-scale, Mark I BWR test facility.

The test pad upon which the toroidal-wetwell sectors are mounted is a reinforced concrete, subgrade pit. The steel-reinforced concrete pad is 0.3 m thick. Beneath this, an integral, reinforced concrete beam, 0.9 by 0.9 m, is placed in line with the main 90-deg sector, trunnion supports. The foundation deflections were conservatively calculated by simultaneously applying about twice the sum of all expected peak loads. All computed deflections were equal to or less than 0.2 mm. This small deflection assures that the test pad offers a rigid base for the toroidal-wetwell sectors.

SCALING RELATIONSHIPS

Scaling relationships are needed so that data obtained may be applied to a full-scale plant. A number of investigators have used dimensional analysis on Mark I pressure-suppression systems to develop relationships that are valid until the bubbles break the water surface in the toroidal wetwell. Morrison (3,4) applied the Buckingham Pi theorem to obtain

$$\frac{F}{\rho g L^3} = \phi\left[\frac{P_i}{\rho g L}, \frac{P_o}{\rho g L}, \frac{RT_o}{gL}, f, \gamma, \frac{t^2 g}{L}\right], \quad (1)$$

where F is force, ρ is liquid density, g is the gravitational constant, L is a characteristic length, P_i and P_o are the initial and applied pressures, respectively, R is the gas constant, T_o is the initial absolute temperature, f is the frictional coefficient, γ is the ratio of gas specific heats, and t is time.

If each of these groupings is held constant for both the model and full-scale plant, then exact scaling is achieved. From a practical standpoint, all groupings except RT_o/gL can be held constant. The characteristic temperature of the full-scale plant is around 300 K. Therefore, if the same gas is utilized, a temperature around 60 K would be required in a 1/5-scale model. Although R can be lowered by using a different gas, normal gases only lower R by a factor of two below that for air. Imperfect scaling still results.

Table 1. Design parameters of major components.

Component and parameter	Full-scale prototype[a]	1/5-scale
Toroidal wetwell		
Maximum internal pressure, kPa	450	450
Major diameter, m	33.99	6.80
Minor inside diameter, m	9.4	1.9
Wall thickness, mm	15.3 (top half) 17.1 (bottom half)	19.0
Drywell		
Volume, m^3	4500	9.77
Maximum internal pressure, kPa	450	790
Vent pipe (90-deg sector)		
Diameter, m	2.06	0.412
Wall thickness, mm	6.4 (minimum)	6.4
Ringheader		
Inside diameter, m	1.45	0.29
	6.4	5.1
Downcomer		
Inside diameter, m	0.61	0.12
Wall thickness, mm	6.4 to 9.52	2.4
Submergence, m	1.2	0.24

[a]Peach Bottom Nuclear Power Plant (1).

Table 2. Summary of transducer accuracy and uncertainty specifications for the 1/5-scale pressure-suppression test.

Type	Number trans-ducers	Range	Transducer response time	Transducer accuracy: Factory stated (lab. conditions)	Transducer accuracy: Anticipated (test conditions)	Expected uncertainty[a]
Pressure	71	0–69 kPa	25 μs	41 Pa	690 Pa	3.4% of $L_{max\downarrow}$
	22	0–520 kPa	25 μs	2.6 kPa	6900 Pa	9.6% of $L_{max\uparrow}$
Differential pressure	3[b]	0–2.5 kPa	1.7 ms	250 Pa	25 Pa	–
	1[b]	0–69 kPa	1 ms	6.9 kPa	690 Pa	–
	3[c]	0–25 kPa	1 ms	2.5 kPa	250 Pa	–
Temperature	38	280–600 K	10 ms	1.7 K	3.4 K	1.2%
Strain gages	21	0.025 mm	1 μs	0.00025 mm	0.0005 mm	4% of ε_{max}
Load cells	5	110 kN		0.56 kN	2.2 kN	6.5% of $L_{max\downarrow}$
	2	450 kN	100 μs	2.2 kN	9.0 kN	18% of $L_{max\uparrow}$
Pool swell	40	–	1 μs	–	3.2 mm	0.5% of PS_{max}
Acceleration	8	25 g	1 ms	0.75 g	0.75 g	–
Displacement	10	10 mm	1 ms	0.08 mm	0.25 mm	–
TOTAL	224					

[a]$L_{max\downarrow}$ = maximum expected downward load, $L_{max\uparrow}$ = maximum expected upward load, ε_{max} = maximum expected strain, and PS_{max} = maximum expected pool swell.

[b]Pitot static

[c]Orifice

In experimental work at Lawrence Livermore Laboratory, air was discharged through a submerged, single downcomer-vent, using 5- and 0.5-litre, spherical flasks (4). Results from these experiments indicate that peak downloads and peak uploads in the toroidal wetwell are scaled equally well by maintaining all groupings constant except for RT_0/gL. In hypotheses used by others (5), f is also varied. The scaling relationships of all investigators are consistent in that, between model and full-scale plant,

$$F \propto L^3 \text{ , } P \propto L\text{, and } t \propto \sqrt{L} \quad . \qquad (2)$$

For this reason, air tests on the 1/5-scale facility were conducted with initial and applied pressures that were 1/5 of those in a full-scale plant. Forces would be 1/125 of those in a full-scale plant and would occur in $1/\sqrt{5}$ the time.

EXPERIMENTAL RESULTS

In a typical test, we first pressurized a selected volume of nitrogen in the storage bottles to a level (between 3.1 and 6.9 MPa) that would produce the desired computer-predicted, drywell pressure-time history. Next, the drywell and toroidal wetwells were evacuated to 1/5 atm (20 kPa). The initial pressure of 1/5-atm permitted data to be scaled to a prototype, initial pressure of 1 atm. All instrumentation recording systems were turned on, and the rupture disks were burst. The test was complete after approximately 20 s, when the pressure in the nitrogen-storage bottles, drywell, and toroidal wetwells had equalized.

Figure 5 shows unfiltered, pressure data from the drywell and 90-deg toroidal wetwell for a nominal test.* The desired, drywell pressure-time history (6), based on a postulated plant-breakflow rate of 22.8 Mg/s, agrees very well with that actually achieved. The pressure in the drywell starts to rise about 3 s after an electronic signal is sent to bleed gas from a rupture-disk assembly that in turn initiates the test.

After the beginning of drywell pressurization, a delay of ~0.1 s occurs before the pressure in the bottom of the toroidal-wetwell water pool starts to rise rapidly. The vents are cleared of water about the time the first peak in the water-pool pressure is reached. Drywell gas from each downcomer then enters the water pool, and the resulting bubbles expand in size until they essentially reach the bottom of the wetwell. Water-pool pressure generally decreases from the first peak until the bubbles break through the pool surface (~3.25 s after initiation) and communicate with the air space above. After this time, the pressures in the water pool, air space, and drywell all increase at the same rate.

Pressure in the air space of the wetwell remains constant until the time of vent clearing. Bubbles injected into the water pool then cause the pool surface to rise and the air space to be compressed. The pressure in the air space continues to rise until the bubbles break through the water surface. By this time, the bubbles have overexpanded, and the pressure inside the bubbles is less than that in the air space. As the bubbles break through, gas rushes from the air space into the bubbles, causing an inflection in the air-space pressure curve. Following bubble breakthrough, the air-space pressure continues to rise at about the same rate as the drywell pressure.

*Nominal, as used in this paper, refers to conditions that are scaled down from those postulated in a prototype BWR plant.

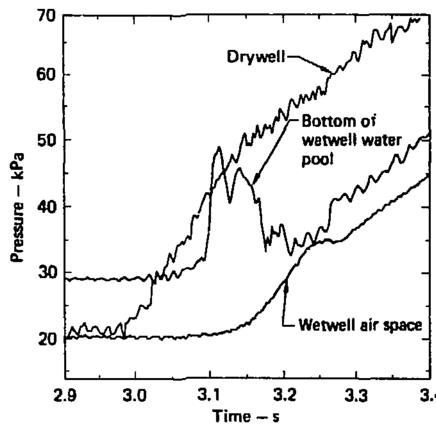

Figure 5. Pressure data (unfiltered) from the drywell and the 90-deg toroidal wetwell sector (nominal test 1.3.1).

Note that at the time of bubble breakthrough (~3.25 s), the pressure in the air space of the wetwell nearly equals that at the bottom of the water pool. This indicates little hydrostatic-pressure head between the two locations at this time and is consistent with the observation from high-speed motion pictures that the bubbles essentially reach the bottom of the toroidal wetwell.

A comparison of the hydrodynamic, vertical-loading function (determined from the integral of the pool-boundary pressure over the surface area) with the response of the 90°-toroidal wetwell (determined from the sum of three external load cells) is shown in Fig. 6. The major events evident on the curves are nearly coincident in time and amplitude – the only difference is that the response oscillates more than the hydrodynamic vertical-loading function. This comparison indicates that the support system of the wetwell permitted peak vertical loads to be measured by either load cells or pressure integration.

The variation of peak vertical load with initial drywell-pressurization rate is shown in Fig. 7. (Peak vertical loads were determined by integration of pressure over internal surface area.) The standard deviation of the linear least-squares fits was, at highest, 4% of the load at a drywell-pressurization rate of 190 kPa/s. Note that the peak download varies considerably more than the peak upload and that these variations are larger for the greater submergence. One explanation for this larger variation of the peak downloads is that the pressure above the water column, as it leaves the downcomers, increases directly with increased, initial drywell-pressurization rate, thereby forcing the water out of the downcomers more rapidly. The peak uploads, occurring at about the time the bubbles break the water surface, are affected more by buoyancy forces.

Figure 8 shows the influence of downcomer submergence on peak vertical loads. The loads were again determined by integration of the pressure over the surface area and were corrected for any test-to-test variation in the nominal value, 190 kPa/s, used for initial drywell pressurization. The grouping of points at the nominal submergence of 0.24 m results from repeated nominal tests. The uploads are influenced less than the downloads by variations in downcomer submergence.

One means of reducing the magnitude of the vertical loads is by introducing initial drywell overpressure. If the initial pressure in the drywell is slightly more than in the toroidal wetwell, the water level inside the downcomers at first will be lower than that outside the downcomers. Figure 9 shows, for nominal values of initial drywell-pressurization rate and downcomer submergence, the sensitivity of peak vertical loads in the 90-deg toroidal wetwell to initial overpressure in the drywell. In our experiment, an initial drywell overpressure of 0.19 m of water reduced the peak download

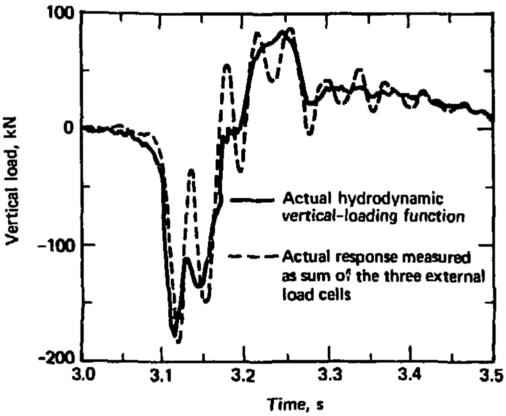

Figure 6. Comparison of the hydrodynamic vertical-loading function with the response of the 90-deg toroidal wetwell (nominal test 1.3.1).

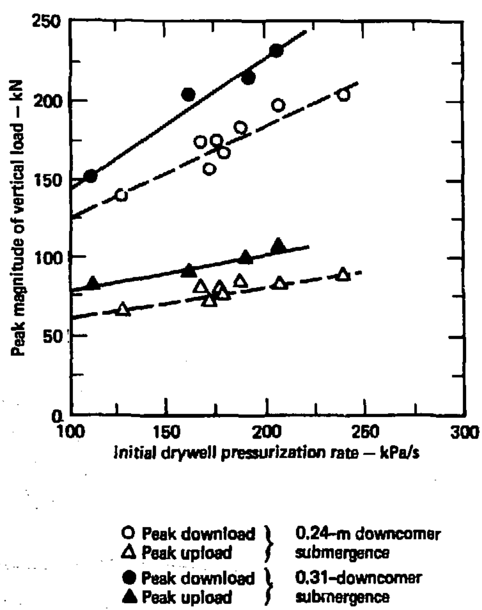

Figure 7. Effect of drywell-pressurization rate on the peak vertical loads on the 90-deg toroidal wetwell.

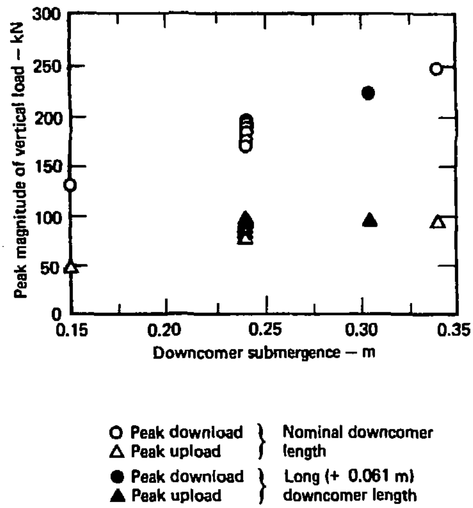

Figure 8. Effect of downcomer submergence on the peak loads on the 90-deg toroidal-wetwell sector.

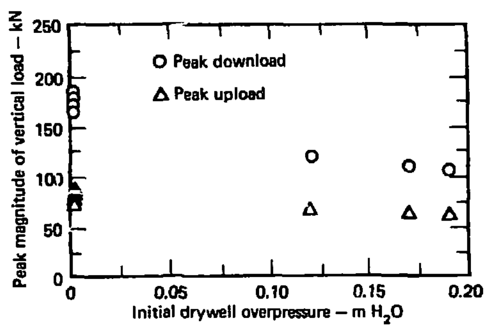

Figure 9. Effect of initial, drywell overpressure on the peak vertical loads on the 90-deg toroidal wetwell as determined by the integral of pressure over the surface area.

and peak upload by about one-half and one-fourth, respectively.

The effects of artificially increasing the vent-line loss coefficient by changing the size of the orifice placed in the vent lines are indicated in Table 3. The nominal-size orifice of 0.241 m in diameter, which we used in most of the tests, was sized to correspond to Moody scaling (5).

A comparison of peak download and upload from these tests reveals that for the larger orifices, the wetwell response, measured as the sum of the three external load cells, varied by 5% or less from the response in the nominal-size orifice tests. A comparison of the peak hydrodynamic load, as determined by integration of the pressure over the internal surface area of the wetwell, showed a corresponding variation of 11% on peak download and 27% on peak upload. Peak downloads were slightly less on tests without orifices. Peak uploads were slightly more.

The small variations in peak downloads and peak uploads with changes in vent-line loss coefficient should be expected. Until the downcomers are cleared of water, the flow of air out of the drywell is small. As a result, the pressure in the downcomers just above the water level is close to the pressure in the drywell, regardless of the magnitude of the vent-line loss coefficient. Because the peak download occurs at about the time the downcomers clear of water, a change in the vent-line loss coefficient should have a small effect. The peak uploads also show small variation with changes in vent-line loss coefficient. These results from the 1/5-scale tests are consistent with earlier results from our bench-top, scaling-law experiments (4).

Table 4 shows normalized, peak vertical forces per downcomer for (a) standard-case tests where the drywell-pressurization rate corresponds to a full-scale plant value of 420 kPa/s, (b) tests where the drywell-pressurization rate of 290 kPa/s, was 30% below standard, and (c) tests where there was a standard pressurization rate but the drywell overpressure corresponded to a full-scale-plant value of 0.92 m of water. All forces were normalized to the peak download present for the nominal case tests. For example, the peak download present for case (b) is 60% of that for case (a).

Table 3. Comparison of peak vertical loads in the 90-deg toroidal wetwell for vent lines restricted with various sizes of orifices.

Vent-line orifice, diameter, m	Peak download, kN		Peak upload, kN	
	Load-cell response	Hydrodynamic load	Load-cell response	Hydrodynamic load
0.241 (Nominal case)	189	177	90	79
0.269	180	166	90	79
0.412 (No orifice — i.d. of vent line)	181	158	94	100

Table 4. Peak vertical forces in terms of normalized force and of force ratio of three-dimensional 90-deg sector to two-dimensional 7.5-deg sector.

Test cases[a]	Peak downward force		Peak upward force	
	Normalized force	3-D/2-D *force ratio*	Normalized *force*	3-D/2-D *force ratio*
(a) Standard test: $\dot{P}_{dw}$ = 420 kPa/s, ΔP_{dw} = 0	1.0	1.1	0.4	1.3
(b) $\dot{P}_{dw}$ = 290 kPa/s, Δ_{dw} = 0	0.6	1.3	0.3	1.3
(c) $\dot{P}_{dw}$ = 420 kPa/s, ΔP_{dw} = 0.92 m-H_2O	0.8	1.1	0.4	1.2

[a]Values of drywell-pressurization rate ($\dot{P}_{dw}$) and drywell overpressure (ΔP_{dw}) are referenced to a full-scale plant.

Because data from both our two-dimensional 7.5-deg sector and our three-dimensional 90-deg sector were obtained in each test, we can separate any three-dimensional effects present. Also shown in Table 4 are three-dimensional or two-dimensional ratios of force. The values are the ratio of peak force per downcomer in the 90-deg sector to the corresponding value in the 7.5-deg sector. As an example, in case (a), the peak upward force in the three-dimensional 90-deg sector is 30% higher than the corresponding value in the two-dimensional 7.5-deg sector. Further details of the test results may be found in Refs. 7 and 8.

CONCLUSIONS

Reproducible and accurate results from 27 air tests show the parameters that most affect peak vertical loads are initial drywell-pressurization rate and downcomer submergence. Utilization of initial drywell overpressure to depress the water level inside the downcomers reduces peak vertical loads. Peak forces occurring in the three-dimensional, 90-deg sector, toroidal wetwell are slightly higher than corresponding forces in the two-dimensional 7.5-deg sector.

Some tests were conducted where the vent-line loss coefficient was varied by changing orifice restrictions. Peak downloads were insensitive to changes in the coefficient, and peak uploads were only slightly affected.

ACKNOWLEDGEMENT

This work was performed under the auspices of the U. S. Department of Energy, under contract No. W-7405-Eng-48.

REFERENCES

(1) Philadelphia Electric Company, "Final Safety Analysis Report, Peach Bottom Atomic Power Station Units No. 2 and 3."

(2) McCauley, E. W. and Pitts, J. H., Principal Investigators, "Mark I 1/5-Scale Boiling Water Reactor Pressure Suppression Facility," compiled and written by R.G. Altes, J.H. Pitts, R.F. Ingrahm, and E.K. Collins, Lawrence Livermore Laboratory, Rept. UCRL-52340 (1977).

(3) Morrison, F. A., Jr., Lawrence Livermore Laboratory, private communication (1976).

(4) McCauley, E. W. and Lai, W., "Air Scaling and Modeling Studies for the 1/5 Scale Mark I Boiling Water Reactor Pressure Suppression Experiment," Lawrence Livermore Laboratory, Report UCRL-52383 (1977).

(5) Moody, F. J., Appendix A of "Mark I, 1/12 Scale Pressure Suppression Pool Swell Tests," by Torbeck, J.E., Galyardt, D.L., and Walter, J.P., General Electric Company, Report NEDE-13456 (1976).

(6) L.S. Slegers, Nuclear Regulatory Commission, private communication (1977).

(7) McCauley, E.W. and Pitts, J.H., Principal Investigators, "Mark I 1/5-Scale Boiling Water Reactor Pressure Suppression Experiment Quick-Look Report," Lawrence Livermore Laboratory, Reports UCID-17446-1 through 17446-6 (Eds. W. Lai and E.K. Collins) and UCID-17446-7 (Eds. W. Lai and R.F. Ingraham) (1977).

(8) McCauley, E.W. and Pitts, J.H., Principal Investigators, "Final Air Test Results for the 1/5-Scale Mark I Boiling Water Reactor Pressure Suppression Experiment" compiled by E.K. Collins and W. Lai, Lawrence Livermore Laboratory, Rept. UCRL-52371 (1977).